Transient wave propagation in reciprocal bi-isotropic media at oblique incidence

Kristensson, Gerhard; Rikte, Sten

1992

Total number of authors:
2

Transient wave propagation in reciprocal bi-isotropic media at oblique incidence

Gerhard Kristensson and Sten Rikte

Gerhard Kristensson and Sten Rikte

Department of Electromagnetic Theory
Lund Institute of Technology
P.O. Box 118
SE-221 00 Lund
Sweden

Abstract

In this paper a new wave splitting is suggested that simplifies the analysis of wave propagation in reciprocal bi-isotropic media. Two different methods to solve the scattering problem are analyzed; the invariant imbedding and the Green function approach. The medium is modeled by constitutive relations in the time domain (time convolutions) and the slab is assumed to be inhomogeneous with respect to the depth. It is showed that the cross-polarized contribution to the reflected field at normal incidence is zero for the general reciprocal inhomogeneous slab. Moreover, the rotation and the attenuation of the wave front are calculated explicitly in the general inhomogeneous slab case. Special attention is paid to normal incidence and to the homogeneous semi-infinite medium.

1 Introduction

The increasing interest in wave propagation phenomena in bi-isotropic (chiral) media is well documented, see, e.g., [7, 22] for a recent overview of the field. This paper is a generalization of the analysis is Ref. [20], where scattering by transient electromagnetic waves of normal incidence was investigated. The incident wave in this paper impinges on the slab at an arbitrary oblique angle and the slab is assumed to be inhomogeneous with respect to the depth. The scattering problem in Ref. [20] was solved by the use of wave splitting techniques [2–4, 23], which have been successfully applied to several different wave propagation problems in the time domain, see [1, 5, 8–11, 14, 16–19, 21, 23, 24].

In this paper a new splitting is adopted, which shows strong affinity to the general wave splitting for Maxwell equations in three dimensions introduced by Weston [24]. The new wave splitting has direct physical interpretations. This is in contrast to the one given in [20], which made it necessary to introduce non-physical kernels in an intermediate step in the calculations. The new splitting has also advantages in the numerical implementations of the problem. Furthermore, with this new splitting, it is possible to show that the inhomogeneous slab has no cross-polarization contribution in the reflected field. This result holds for normal incidence with an arbitrary reciprocal inhomogeneous (with respect to depth) slab and therefore generalizes the results from the homogeneous slab case. Moreover, the rotation and the attenuation of the wave front can be calculated in the general inhomogeneous slab case at oblique incidence. Specifically, this result gives the wave front behavior of the transmitted field.

2 Basic equations

The aim of this paper is to investigate electromagnetic wave propagation in the time domain in a reciprocal bi-isotropic medium. The medium is a slab bounded by the surfaces $z = 0$ and $z = L$, respectively, see Figure 1. Outside the slab, ($z < 0$ and $z > L$), the medium is assumed to be homogeneous with constant permittivity $\epsilon_0 \epsilon$

and permeability $\mu_0\mu$. For simplicity these constant values of the permittivity and permeability hold throughout the space. Generalization of this problem to phase velocity mismatch at the boundaries of the slab is not considered in this paper, c.f. [18].

Due to the slab geometry it is pertinent to rewrite the fields in a transverse and a perpendicular part with respect to the slab interface. Specifically, introduce the following notation:

$$\boldsymbol{E}(\boldsymbol{r},t) = \boldsymbol{E}_\parallel(\boldsymbol{r},t) + \hat{z}E_z(\boldsymbol{r},t)$$

and

$$\nabla = \nabla_\parallel + \hat{z}\frac{\partial}{\partial z}$$

where

$$\boldsymbol{E}_\parallel(\boldsymbol{r},t) = \hat{z} \times (\boldsymbol{E}(\boldsymbol{r},t) \times \hat{z})$$

and similarly for all other vector fields. Throughout this paper a 2×2 matrix notation is adopted and all such matrices are typed in upright boldface and vectors in slanted boldface[1]. Furthermore, no distinction is made between vectors and their representation as column vectors of cartesian coordinates in this paper.

The Maxwell equations are the basic equations that model the dynamics of the electromagnetic fields.

$$\begin{cases} \nabla \times \boldsymbol{E}(\boldsymbol{r},t) = -\dfrac{\partial \boldsymbol{B}(\boldsymbol{r},t)}{\partial t} \\ \nabla \times \boldsymbol{H}(\boldsymbol{r},t) = \dfrac{\partial \boldsymbol{D}(\boldsymbol{r},t)}{\partial t} \end{cases}$$

The x- and y-components of Maxwell equations can be written as

$$\frac{\partial}{\partial z}\begin{pmatrix} \mathbf{J}\boldsymbol{E}_\parallel \\ \mathbf{J}\boldsymbol{H}_\parallel \end{pmatrix} = \frac{\partial}{\partial t}\begin{pmatrix} -\boldsymbol{B}_\parallel \\ \boldsymbol{D}_\parallel \end{pmatrix} + \begin{pmatrix} \mathbf{J}\nabla_\parallel E_z \\ \mathbf{J}\nabla_\parallel H_z \end{pmatrix}$$

The 2×2 matrix $\mathbf{J}$ is defined as the constant matrix

$$\mathbf{J} = \begin{pmatrix} 0 & -1 \\ 1 & 0 \end{pmatrix}$$

Notice that the matrix $\mathbf{J}$, considered as an operator on the vectors in the x-y-plane, can be written as

$$\mathbf{J} = \hat{z} \times \mathbf{I}$$

where the 2×2 identity matrix $\mathbf{I}$ is

$$\mathbf{I} = \begin{pmatrix} 1 & 0 \\ 0 & 1 \end{pmatrix}$$

and, therefore, the matrix $\mathbf{J}$ is a rotation of $-\pi/2$ around the z-axis. Notice also that

$$\mathbf{J}\mathbf{J} = -\mathbf{I}$$

---

[1]At a few occasions 4×4 matrices are introduced. They are also written on upright boldface. From the context it is obvious whether a 2×2 or a 4×4 matrix is regarded.

The z-components of the Maxwell equations are also used.

$$\frac{\partial}{\partial t}\begin{pmatrix} -B_z \\ D_z \end{pmatrix} = \begin{pmatrix} \partial_x E_y - \partial_y E_x \\ \partial_x H_y - \partial_y H_x \end{pmatrix}$$

It is appropriate to rewrite the x- and y-components of the Maxwell equations as

$$\frac{\partial}{\partial z}\begin{pmatrix} \boldsymbol{E}_\parallel \\ \eta\mathbf{J}\boldsymbol{H}_\parallel \end{pmatrix} = \frac{1}{c}\frac{\partial}{\partial t}\begin{pmatrix} c\mathbf{J}\boldsymbol{B}_\parallel \\ c\eta\boldsymbol{D}_\parallel \end{pmatrix} + \begin{pmatrix} \nabla_\parallel E_z \\ \eta\mathbf{J}\nabla_\parallel H_z \end{pmatrix} \tag{2.1}$$

and the z-components as

$$\frac{1}{c}\frac{\partial}{\partial t}\begin{pmatrix} cB_z \\ c\eta D_z \end{pmatrix} = \begin{pmatrix} -(\mathbf{J}\nabla_\parallel)^t & 0 \\ 0 & -(\nabla_\parallel)^t \end{pmatrix}\begin{pmatrix} \boldsymbol{E}_\parallel \\ \eta\mathbf{J}\boldsymbol{H}_\parallel \end{pmatrix} \tag{2.2}$$

where

$$\begin{pmatrix} -(\mathbf{J}\nabla_\parallel)^t & 0 \\ 0 & -(\nabla_\parallel)^t \end{pmatrix} = \begin{pmatrix} \partial_y & -\partial_x & 0 & 0 \\ 0 & 0 & -\partial_x & -\partial_y \end{pmatrix}$$

and the phase velocity c and the wave impedance η are

$$c = \frac{1}{\sqrt{\epsilon_0\epsilon\mu_0\mu}} = \frac{c_0}{\sqrt{\epsilon\mu}}$$

$$\eta = \sqrt{\frac{\mu_0\mu}{\epsilon_0\epsilon}} = \eta_0\sqrt{\frac{\mu}{\epsilon}}$$

The permittivity, permeability, wave impedance and phase velocity of vacuum are denoted ϵ_0, μ_0, η_0 and c_0, respectively. The constants ϵ and μ are the relative permittivity and permeability, respectively, of the medium. The form of the Maxwell equations in (2.1) and (2.2) is appropriate for the analysis below.

The constitutive relations model the dynamics of the constitutive charges of the medium. In Ref. [12] (see also [13]) it was proven, under very general assumptions, that the constitutive relations must be of the form of time convolutions. In this paper a slightly altered version of these constitutive relations is used (for a relation between the two different versions, see Appendix A). The constitutive relations that are appropriate for the treatment in this paper are

$$\begin{cases} c\eta\boldsymbol{D}(\boldsymbol{r},t) = \boldsymbol{E}(\boldsymbol{r},t) + (G*\boldsymbol{E})(\boldsymbol{r},t) + \eta(K*\boldsymbol{H})(\boldsymbol{r},t) \\ c\boldsymbol{B}(\boldsymbol{r},t) = -(K*\boldsymbol{E})(\boldsymbol{r},t) + \eta\boldsymbol{H}(\boldsymbol{r},t) + \eta(F*\boldsymbol{H})(\boldsymbol{r},t) \end{cases} \tag{2.3}$$

where time convolution is denoted by a $*$, i.e.,

$$(G*\boldsymbol{E})(\boldsymbol{r},t) = \int_{-\infty}^{t} G(\boldsymbol{r},t-t')\boldsymbol{E}(\boldsymbol{r},t')\,dt'$$

The kernels G and F model the ordinary dispersive effects in the absence of bi-isotropy. The kernel K is a measure of the bi-isotropy of the medium. Notice that the kernel K appears in both equations in the constitutive relations and therefore the medium is reciprocal [13]. The kernels G, F and K are zero for $t < 0$ due to

causality. Furthermore, these kernels are assumed to be continuously differentiable functions of t for $t > 0$ for each $\boldsymbol{r}$.

In Section 3 the inverse of the constitutive relations in (2.3) are also used. To avoid cumbersome notation it is therefore convenient to introduce the inverse of (2.3) explicitly. The inverse of (2.3) is

$$\begin{cases} \boldsymbol{E}(\boldsymbol{r},t) = c\eta\boldsymbol{D}(\boldsymbol{r},t) + c\eta(g*\boldsymbol{D})(\boldsymbol{r},t) + c(k*\boldsymbol{B})(\boldsymbol{r},t) \\ \eta\boldsymbol{H}(\boldsymbol{r},t) = -c\eta(k*\boldsymbol{D})(\boldsymbol{r},t) + c\boldsymbol{B}(\boldsymbol{r},t) + c(f*\boldsymbol{B})(\boldsymbol{r},t) \end{cases} \tag{2.4}$$

where the three new kernels g, f and k are defined in terms of the original kernels G, F and K as

$$\begin{cases} k + (F + G + G*F + K*K)*k = -K \\ g + G + g*G = k*K \\ f + F + f*F = k*K \end{cases} \tag{2.5}$$

From these equations it is immediately clear that the first equation determines the kernel k uniquely, since it is a Volterra equation of the second kind in k. With the same arguments the second and third equations uniquely determine the kernels g and f, respectively. Conversely, it is also clear that G, F and K can be recovered from g, f and k. This is easily seen from the equations in (2.5), which imply that

$$K + (f + g + g*f + k*k)*K = -k$$

This is again a Volterra equation of the second kind in K if g, f and k are known. The kernels G and F can then be computed from the second and the third equations in (2.5), respectively.

3   Oblique incidence

The analysis and the equations in Section 2 are general. No assumption about the material has been made so far. In this section certain assumptions are made to handle the oblique incidence case. It is assumed that the slab is inhomogeneous only with depth z. The susceptibility kernels are therefore functions of z and t, i.e., $G(\boldsymbol{r},t) = G(z,t)$ and similarly for all other susceptibility kernels. The geometry of the problem is depicted in Figure 1. All fields are assumed to vary as a function of space $\boldsymbol{r}$ and time t as

$$\boldsymbol{E}(\boldsymbol{r},t) = \hat{x}E_x(z,s) + \hat{y}E_y(z,s) + \hat{z}E_z(z,s)$$
$$\boldsymbol{H}(\boldsymbol{r},t) = \hat{x}H_x(z,s) + \hat{y}H_y(z,s) + \hat{z}H_z(z,s)$$

where

$$s = t - \frac{y\sin\theta}{c}$$

and θ is the angle of incidence. The fields are only functions of depth z and the time coordinate $s = t - y\sin\theta/c$. This assumption implies that the fields at a certain point and time $(\boldsymbol{r},t)$ is identical to the fields at an earlier time $t - y\sin\theta/c$ at the

point $y = 0$ and depth z. Therefore, at constant depth z, the history of the fields is translated in time with $y \sin \theta / c$. The time convolutions in the constitutive relations, (2.3), are changed

$$(G * \boldsymbol{E})(\boldsymbol{r}, t) = \int_{-\infty}^{t} G(z, t - t') \boldsymbol{E}(z, t' - y \sin \theta / c) \, dt' = \int_{-\infty}^{s} G(z, s - s') \boldsymbol{E}(z, s') \, ds'$$

These assumptions imply that all derivatives in the Maxwell equations are simplified.

$$\partial_x = \frac{\partial}{\partial x} = 0, \quad \partial_t = \frac{\partial}{\partial t} = \partial_s, \quad \partial_y = \frac{\partial}{\partial y} = -\frac{\sin \theta}{c} \partial_s$$

and the Maxwell equations (2.1) with the constitutive relations (2.3) imply that the x- and y-components satisfy

$$c \frac{\partial}{\partial z} \begin{pmatrix} \boldsymbol{E}_{\parallel} \\ \eta \mathbf{J} \boldsymbol{H}_{\parallel} \end{pmatrix} = \begin{pmatrix} -K * \mathbf{J} & (1 + F*) \mathbf{I} \\ (1 + G*) \mathbf{I} & -K * \mathbf{J} \end{pmatrix} \frac{\partial}{\partial s} \begin{pmatrix} \boldsymbol{E}_{\parallel} \\ \eta \mathbf{J} \boldsymbol{H}_{\parallel} \end{pmatrix} - \sin \theta \frac{\partial}{\partial s} \begin{pmatrix} 0 \\ E_z \\ -\eta H_z \\ 0 \end{pmatrix}$$
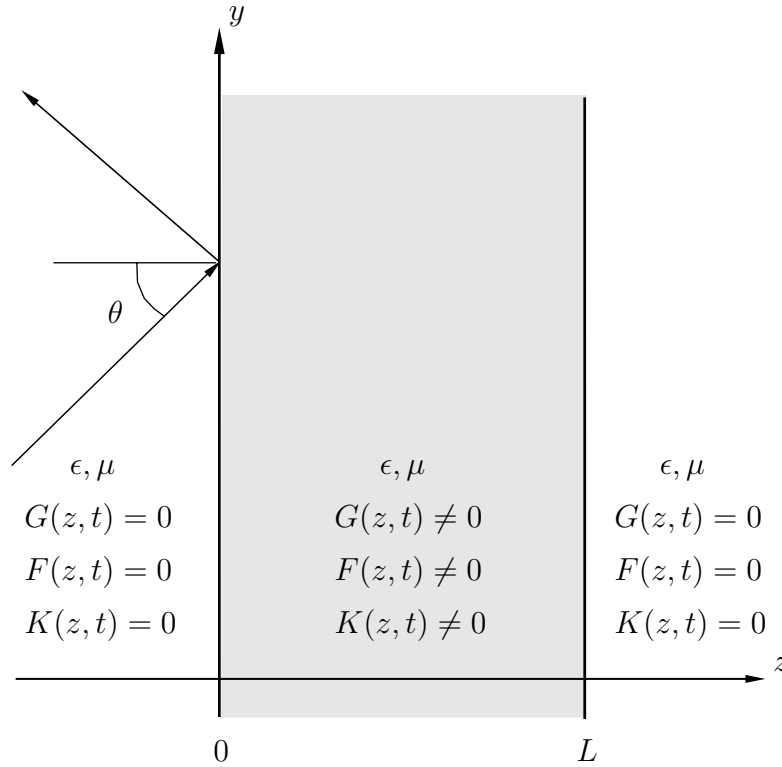

Figure 1: Geometry of the problem.

The z-components of the fields in the last term are now eliminated. The constitutive relations (2.4) and the Maxwell equations (2.2) imply that the z-components

of the fields satisfy

$$\frac{\partial}{\partial s}\begin{pmatrix} E_z \\ \eta H_z \end{pmatrix} = \begin{pmatrix} k* & 1+g* \\ 1+f* & -k* \end{pmatrix} \frac{\partial}{\partial s}\begin{pmatrix} cB_z \\ c\eta D_z \end{pmatrix}$$

$$= -\sin\theta \begin{pmatrix} k* & 1+g* \\ 1+f* & -k* \end{pmatrix}\begin{pmatrix} 1 & 0 & 0 & 0 \\ 0 & 0 & 0 & -1 \end{pmatrix}\frac{\partial}{\partial s}\begin{pmatrix} \boldsymbol{E}_\| \\ \eta\boldsymbol{JH}_\| \end{pmatrix}$$

Thus, it is possible to eliminate the z-components and obtain an equation in the transverse components of the electric and the magnetic fields only. The result is

$$c\frac{\partial}{\partial z}\begin{pmatrix} \boldsymbol{E}_\| \\ \eta\boldsymbol{JH}_\| \end{pmatrix} = \begin{pmatrix} -K*\boldsymbol{J} & (1+F*)\boldsymbol{I} \\ (1+G*)\boldsymbol{I} & -K*\boldsymbol{J} \end{pmatrix}\frac{\partial}{\partial s}\begin{pmatrix} \boldsymbol{E}_\| \\ \eta\boldsymbol{JH}_\| \end{pmatrix}$$

$$+ \sin^2\theta \begin{pmatrix} 0 & 0 & 0 & 0 \\ k* & 0 & 0 & -1-g* \\ -1-f* & 0 & 0 & -k* \\ 0 & 0 & 0 & 0 \end{pmatrix}\frac{\partial}{\partial s}\begin{pmatrix} \boldsymbol{E}_\| \\ \eta\boldsymbol{JH}_\| \end{pmatrix} \tag{3.1}$$

The second term on the right hand side vanishes at normal incidence. Note that the first term on the right hand side contains the constitutive relations, (2.3), and the second term contains the constitutive relations given by (2.4).

4   Wave splitting

In this section the new wave splitting for the bi-isotropic medium is introduced. The idea of wave splitting has been used in several scattering problems [2–4, 23]. The wave splitting used in this paper has several similarities with the three-dimensional wave splitting for the Maxwell equations suggested by Weston [24].

Mathematically, the wave splitting is a change in the dependent variables. The definition is

$$\begin{pmatrix} \boldsymbol{E}^+(z,s) \\ \boldsymbol{E}^-(z,s) \end{pmatrix} = \mathbf{P}\begin{pmatrix} \boldsymbol{E}_\|(z,s) \\ \eta\boldsymbol{JH}_\|(z,s) \end{pmatrix} \tag{4.1}$$

where the 4×4 matrix $\mathbf{P}$ is defined as

$$\mathbf{P} = \frac{1}{2\cos\theta}\begin{pmatrix} \cos\theta\mathbf{I} & -\mathbf{SS} \\ \cos\theta\mathbf{I} & \mathbf{SS} \end{pmatrix}$$

with inverse

$$\mathbf{P}^{-1} = \begin{pmatrix} \mathbf{I} & \mathbf{I} \\ -\cos\theta\mathbf{S}^{-1}\mathbf{S}^{-1} & \cos\theta\mathbf{S}^{-1}\mathbf{S}^{-1} \end{pmatrix}$$

The 2×2 matrices $\mathbf{S}$, $\mathbf{I}$ and $\mathbf{J}$ are

$$\mathbf{S} = \begin{pmatrix} 1 & 0 \\ 0 & \cos\theta \end{pmatrix}, \qquad \mathbf{I} = \begin{pmatrix} 1 & 0 \\ 0 & 1 \end{pmatrix}, \qquad \mathbf{J} = \begin{pmatrix} 0 & -1 \\ 1 & 0 \end{pmatrix} \tag{4.2}$$

Notice that $\mathbf{S}$ and $\mathbf{J}$ do not commute.

In these new fields, $\boldsymbol{E}^+(z,s)$ and $\boldsymbol{E}^-(z,s)$, the transverse electric and magnetic fields are

$$\begin{cases} \boldsymbol{E}_\parallel(z,s) = \boldsymbol{E}^+(z,s) + \boldsymbol{E}^-(z,s) \\ \boldsymbol{H}_\parallel(z,s) = \dfrac{1}{\eta}\cos\theta\, \mathbf{J}\mathbf{S}^{-1}\mathbf{S}^{-1}\left(\boldsymbol{E}^+(z,s) - \boldsymbol{E}^-(z,s)\right) \end{cases}$$

Compared to the wave splitting employed in Ref. [20], this new splitting has the advantage that the fields $\boldsymbol{E}^+(z,s)$ and $\boldsymbol{E}^-(z,s)$ are continuous over the slab boundaries. This property facilitates the treatment of the scattering problem.
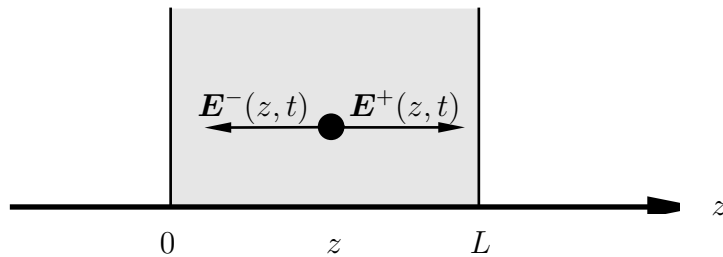

Figure 2: The wave splitting.

Outside the slab, i.e., $z < 0$ and $z > L$, where

$$\begin{cases} \boldsymbol{D}(z,t) = \epsilon\epsilon_0 \boldsymbol{E}(z,t) \\ \boldsymbol{B}(z,t) = \mu\mu_0 \boldsymbol{H}(z,t) \end{cases}$$

the fields $\boldsymbol{E}^+(z,s)$ and $\boldsymbol{E}^-(z,s)$ represent the right and the left going parts of the solution, respectively. More specifically,

$$\begin{cases} \boldsymbol{E}^+(z,s) = \boldsymbol{f}_\parallel(s - z\cos\theta/c) \\ \boldsymbol{E}^-(z,s) = \boldsymbol{g}_\parallel(s + z\cos\theta/c) \end{cases}$$

where $\boldsymbol{f}$ and $\boldsymbol{g}$ are the electric fields of the general plane waves propagating in the direction of incidence and reflection, respectively, see also (5.1). The definition (4.1), however, is well defined even inside the medium where $G \neq 0$, $F \neq 0$ and $K \neq 0$, see also Figure 2 and a formal picture of the wave splitting.

5   Dynamics

The transverse components of the electric and the magnetic fields satisfy the system of equations in (3.1). The plus and minus fields $\boldsymbol{E}^+(z,s)$ and $\boldsymbol{E}^-(z,s)$, defined in Section 4, satisfy similar system of equations. These equations are equivalent to (3.1) and straightforward to derive using (3.1) and (4.1).

$$\begin{aligned} v\frac{\partial}{\partial z}\begin{pmatrix}\boldsymbol{E}^+\\\boldsymbol{E}^-\end{pmatrix} &= \begin{pmatrix}-\mathbf{I} & \mathbf{0}\\\mathbf{0} & \mathbf{I}\end{pmatrix}\frac{\partial}{\partial s}\begin{pmatrix}\boldsymbol{E}^+\\\boldsymbol{E}^-\end{pmatrix}\\ &\quad + \begin{pmatrix}\mathbf{S} & \mathbf{0}\\\mathbf{0} & \mathbf{S}\end{pmatrix}\begin{pmatrix}\boldsymbol{\alpha} & \boldsymbol{\beta}\\\boldsymbol{\gamma} & \boldsymbol{\delta}\end{pmatrix}\begin{pmatrix}\mathbf{S}^{-1} & \mathbf{0}\\\mathbf{0} & \mathbf{S}^{-1}\end{pmatrix} * \frac{\partial}{\partial s}\begin{pmatrix}\boldsymbol{E}^+\\\boldsymbol{E}^-\end{pmatrix} \end{aligned} \tag{5.1}$$

where the longitudinal phase velocity v is

$$v = c/\cos\theta$$

and the 2×2 matrix kernels $\boldsymbol{\alpha}$, $\boldsymbol{\beta}$, $\boldsymbol{\gamma}$ and $\boldsymbol{\delta}$ are

$$\begin{pmatrix} \boldsymbol{\alpha} & \boldsymbol{\beta} \\ \boldsymbol{\gamma} & \boldsymbol{\delta} \end{pmatrix} = \mathbf{X} + \mathbf{Y} \tag{5.2}$$

The 4×4 matrix kernels $\mathbf{X}$, $\mathbf{Y}$ are defined as

$$\mathbf{X} = \frac{1}{2\cos^2\theta} \begin{pmatrix} -\mathbf{G} - \mathbf{F} - 2\mathbf{K} & -\mathbf{G} + \mathbf{F} \\ \mathbf{G} - \mathbf{F} & \mathbf{G} + \mathbf{F} - 2\mathbf{K} \end{pmatrix} \tag{5.3}$$

and

$$\mathbf{Y} = \frac{\tan^2\theta}{2} \begin{pmatrix} f & -k - K & f & k - K \\ k + K & g & k - K & -g \\ -f & k - K & -f & -k - K \\ k - K & g & k + K & -g \end{pmatrix} \tag{5.4}$$

where

$$\mathbf{G} = G\mathbf{SS}, \quad \mathbf{F} = F\cos^2\theta\mathbf{S}^{-1}\mathbf{S}^{-1}, \quad \mathbf{K} = K\mathbf{J}$$

The terms in equation (5.1) are organized such that the term containing the 4×4 matrix $\mathbf{Y}$ vanishes at normal incidence, $\theta = 0$. Both the 4×4 matrices $\mathbf{X}$ and $\mathbf{Y}$ contain the generalized sucseptibility kernels and vanish if there is no slab, i.e., $G(t) = F(t) = K(t) = 0$. The first term gives the dynamics for the free space contribution.

6 Propagation of the wave front

Before the general scattering problem is addressed, it is interesting to analyze the propagation of singularities in the bi-isotropic medium. This analysis gives information about the rotation and the attenuation of the wave front as it propagates through the medium. Specifically, the wave front of the transmitted field can be explicitly given in terms of the incident field. In Appendix B a general derivation of the problem is given.

The propagation of singularities in the positive z-direction for the dynamic system (5.1) depends on the matrix $\boldsymbol{\alpha}(z, +0)$.

$$\boldsymbol{\alpha}(z, +0) = \frac{1}{2\cos^2\theta}(-\mathbf{G} - \mathbf{F} - 2\mathbf{K})(z, +0) + \frac{\tan^2\theta}{2}\begin{pmatrix} f & -k - K \\ k + K & g \end{pmatrix}(z, +0)$$

$$= \frac{1}{2\cos^2\theta}\begin{pmatrix} -G - F & 2K \\ -2K & -G - F \end{pmatrix}(z, +0)$$

This is the upper left corner contribution on the right hand side of (5.1). Moreover, in the simplification of this result, equation (2.5) has been used. The other matrices

$\boldsymbol{\beta}$, $\boldsymbol{\gamma}$ and $\boldsymbol{\delta}$ play no rôle in the propagation of the wave front in the positive z-direction.

Assume there is a finite jump discontinuity in the plus field $\boldsymbol{E}^+$ at $z = 0$. This finite jump discontinuity propagates through the medium and the finite jump discontinuity at depth z is related to its value at $z = 0$ as

$$\left[\boldsymbol{E}^+(z, s + z/v)\right] = \mathbf{Q}'(0, z)\left[\boldsymbol{E}^+(0, s)\right]$$

where the 2×2 matrix $\mathbf{Q}'(0, z)$ quantifies the rotation and the attenuation of the discontinuity. The square bracket $\left[\boldsymbol{E}^+(z, s + z/v)\right]$ denotes the finite jump discontinuity of the field at the point $(z, s + z/v)$. The field $\boldsymbol{E}^-$ shows no finite jump discontinuity of this kind and therefore the total field $\boldsymbol{E}$ has exactly the same finite jump discontinuity as the field $\boldsymbol{E}^+$ above. Notice also, that the finite jump discontinuity $\left[\boldsymbol{E}^+(0, s)\right]$ is the same on either side of the interface of the slab.

The matrix $\mathbf{Q}'(0, z)$ satisfies the following first order differential equation found by use of propagation of singularity arguments.

$$\frac{d}{dz}\mathbf{Q}'(0, z) = \frac{1}{v}\mathbf{S}\boldsymbol{\alpha}(z, +0)\mathbf{S}^{-1}\mathbf{Q}'(0, z)$$
$$\mathbf{Q}'(0, 0) = \mathbf{I}$$

To solve this system of equations it is convenient to introduce a new matrix

$$\mathbf{Q} = \mathbf{S}^{-1}\mathbf{Q}'\mathbf{S}$$

i.e., the matrix $\mathbf{Q}'$ is similarity transformed. The matrix $\mathbf{Q}$ satisfies a simpler initial value problem.

$$\frac{d}{dz}\mathbf{Q}(0, z) = \frac{1}{v}\boldsymbol{\alpha}(z, +0)\mathbf{Q}(0, z) = \frac{\cos\theta}{c}\boldsymbol{\alpha}(z, +0)\mathbf{Q}(0, z)$$
$$\mathbf{Q}(0, 0) = \mathbf{I}$$

This matrix equation can be explicitly solved and expressed in the following general notation:

$$\mathbf{Q}(z_1, z_2) = e^{-\frac{1}{2c\cos\theta}\int_{z_1}^{z_2}(G(z', +0) + F(z', +0))\, dz'}\begin{pmatrix} \cos\phi(z_1, z_2) & -\sin\phi(z_1, z_2) \\ \sin\phi(z_1, z_2) & \cos\phi(z_1, z_2) \end{pmatrix}$$

where the angle of rotation of the wave front $\phi(z_1, z_2)$ is

$$\phi(z_1, z_2) = -\frac{1}{c\cos\theta}\int_{z_1}^{z_2} K(z', 0)\, dz' \tag{6.1}$$

Notice that this result holds for an inhomogeneous slab with arbitrary susceptibility kernels $G(z, t)$, $F(z, t)$ and $K(z, t)$.

The matrix $\mathbf{Q}'$ will play an important part in the definition of the imbedding kernels and the Green functions in (7.1) and (11.1), respectively.

7 Scattering operators

The reflection and the transmission kernels of the slab give the impulse response on both sides of the slab for an excitation from the left, i.e., the reflected and the transmitted field, respectively, for a delta pulse excitation.

The imbedding approach to solve the scattering problem uses the idea of studying a one-parameter family of problems. At one end of the parameter interval the scattering problem is trivial while for the other endpoint of the parameter interval the full scattering problem is solved. This idea has been used extensively to solve scattering problems in the time domain during the last decade [1, 2, 4, 5, 9–11, 15–20, 23].
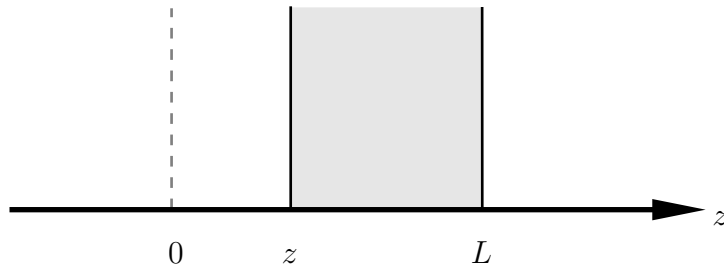

Figure 3: The imbedding geometry.

Consider a subsection $[z, L]$ of the physical slab $[0, L]$, see Figure 3. The relation between the fields $\boldsymbol{E}^+(z, s)$, $\boldsymbol{E}^-(z, s)$ and $\boldsymbol{E}^+(z, s)$, $\boldsymbol{E}^+(L, s+(L-z)/v)$, respectively, are given by the following definitions (for more details of how these relations are derived, see [4, 6]):

$$\begin{cases} \boldsymbol{E}^-(z, s) = \left(\mathbf{R}'(z, \cdot) * \boldsymbol{E}^+(z, \cdot)\right)(s) \\ \boldsymbol{E}^+(L, s + (L - z)/v) = \mathbf{Q}'(z, L)\left\{\boldsymbol{E}^+(z, s) + \left(\mathbf{T}'(z, \cdot) * \boldsymbol{E}^+(z, \cdot)\right)(s)\right\} \end{cases} \quad (7.1)$$

where the time convolutions are defined as

$$\left(\mathbf{R}'(z, \cdot) * \boldsymbol{E}^+(z, \cdot)\right)(s) = \int_{-\infty}^{s} \mathbf{R}'(z, s - s')\boldsymbol{E}^+(z, s')\, ds'$$

and the matrix-valued kernels $\mathbf{R}'$ and $\mathbf{T}'$ are

$$\mathbf{R}'(z, s) = \begin{pmatrix} R_{11}(z, s) & R_{12}(z, s)/\cos\theta \\ R_{12}(z, s)\cos\theta & R_{22}(z, s) \end{pmatrix}$$

$$\mathbf{T}'(z, t) = \begin{pmatrix} T_{11}(z, s) & T_{12}(z, s)/\cos\theta \\ T_{21}(z, s)\cos\theta & T_{22}(z, s) \end{pmatrix}$$

Note that the kernel $\mathbf{R}'(z, s)$ has identical off-diagonal entries (apart from the $\cos\theta$ factor). This follows from a more general Ansatz due to the reciprocal nature of the problem. In the second equation in (7.1) a delta measure has been subtracted from the scattering kernel. Thus, the precursors are determined by the remaining part $\mathbf{T}'$.

These kernels, $\mathbf{R}'$ and $\mathbf{T}'$, can physically be interpreted as the reflection and transmission imbedding kernels for the subsection $[z, L]$ of the slab. They are defined in the region $(z, s) \in [0, L] \times (-\infty, \infty)$ and are referred to as imbedding kernels. Note that the kernels $\mathbf{R}'(0, s)$ and $\mathbf{T}'(0, s)$ are the physical scattering kernels of the slab and that the kernels $\mathbf{R}'(L, s)$ and $\mathbf{T}'(L, s)$ are zero since the fields $\boldsymbol{E}^{\pm}$ are continuous at $z = L$ (no scatterer is present as $z = L$). Moreover, $\mathbf{R}'(z, s)$ and $\mathbf{T}'(z, s)$ are zero for $s < 0$ due to causality.

To simplify the equations below, it is convenient to use the matrix $\mathbf{S}$, see (4.2), explicitly and to introduce reflection and transmission kernels $\mathbf{R}$ and $\mathbf{T}$.

$$\mathbf{R}(z, s) = \mathbf{S}^{-1}\mathbf{R}'(z, s)\mathbf{S} = \begin{pmatrix} R_{11}(z, s) & R_{12}(z, s) \\ R_{12}(z, s) & R_{22}(z, s) \end{pmatrix}$$

and

$$\mathbf{T}(z, s) = \mathbf{S}^{-1}\mathbf{T}'(z, s)\mathbf{S} = \begin{pmatrix} T_{11}(z, s) & T_{12}(z, s) \\ T_{21}(z, s) & T_{22}(z, s) \end{pmatrix}$$

The transformation with $\mathbf{S}$ is a similarity transformation.

The imbedding kernels $\mathbf{R}$ and $\mathbf{T}$ are equal to zero for $s < 0$ and have finite jump discontinuities at $s = 0$. $\mathbf{T}$ is continuously differentiable for $s > 0$ and so is $\mathbf{R}$ except on the line $s = 2(L - z)/v$, where $\mathbf{R}$ has a finite jump discontinuity.

The imbedding kernels $\mathbf{R}(z, s)$ and $\mathbf{T}(z, s)$ satisfy partial differential equations. These equations, the imbedding equations, will be presented in the next section as well as the finite jump discontinuities of the kernels.

8 The imbedding equations

The imbedding equations are easily derived from the dynamic equation (5.1) and the definition of the imbedding kernels (7.1), see also (B.3) and (B.4) in Appendix B. The result, valid for $s > 0$, $0 < z < L$ and $s \neq 2(L - z)/v$, is

$$v\partial_z\mathbf{R} - 2\partial_s\mathbf{R} = \partial_s\{\boldsymbol{\gamma} + \boldsymbol{\delta} * \mathbf{R} - \mathbf{R} * \boldsymbol{\alpha} - \mathbf{R} * \boldsymbol{\beta} * \mathbf{R}\} \tag{8.1}$$

$$v\partial_z\mathbf{T} = \boldsymbol{\alpha}(z, +0)\mathbf{T} - \partial_s\{\boldsymbol{\alpha} + \boldsymbol{\beta} * \mathbf{R} + \mathbf{T} * \boldsymbol{\alpha} + \mathbf{T} * \boldsymbol{\beta} * \mathbf{R}\} \tag{8.2}$$

$$\mathbf{R}(L, s) = \mathbf{0}$$

$$\mathbf{T}(L, s) = \mathbf{0}$$

$$\mathbf{R}(z, +0) = -\frac{1}{2}\boldsymbol{\gamma}(z, +0)$$

where the four matrices $\boldsymbol{\alpha}$, $\boldsymbol{\beta}$, $\boldsymbol{\gamma}$ and $\boldsymbol{\delta}$ are defined in (5.2), (5.3) and (5.4). Note that the imbedding equations are matrix equations and that the matrices $\boldsymbol{\alpha}$, $\boldsymbol{\beta}$, $\boldsymbol{\gamma}$

and $\boldsymbol{\delta}$ have only six independent elements. These are

$$
\begin{cases}
\alpha_{11} = -\delta_{11} = \dfrac{1}{2\cos^2\theta}(-G - F\cos^2\theta + f\sin^2\theta) \\[2mm]
\beta_{11} = -\gamma_{11} = \dfrac{1}{2\cos^2\theta}(-G + F\cos^2\theta + f\sin^2\theta) \\[2mm]
\alpha_{22} = -\delta_{22} = \dfrac{1}{2\cos^2\theta}(-G\cos^2\theta - F + g\sin^2\theta) \\[2mm]
\beta_{22} = -\gamma_{22} = \dfrac{1}{2\cos^2\theta}(-G\cos^2\theta + F - g\sin^2\theta) \\[2mm]
\alpha_{12} = -\alpha_{21} = \delta_{12} = -\delta_{21} = \dfrac{1}{2\cos^2\theta}(2K - (k + K)\sin^2\theta) \\[2mm]
\beta_{12} = \beta_{21} = \gamma_{12} = \gamma_{21} = \dfrac{1}{2\cos^2\theta}((k - K)\sin^2\theta)
\end{cases}
$$

The value of the matrices at $s = 0$ can be simplified by using (2.5). The result is

$$
\begin{cases}
\boldsymbol{\alpha}(z, +0) = \dfrac{1}{2\cos^2\theta}\begin{pmatrix} -G - F & 2K \\ -2K & -G - F \end{pmatrix}(z, +0) \\[4mm]
\boldsymbol{\beta}(z, +0) = -\dfrac{1}{2\cos^2\theta}\begin{pmatrix} G - F\cos 2\theta & 2K\sin^2\theta \\ 2K\sin^2\theta & G\cos 2\theta - F \end{pmatrix}(z, +0) \\[4mm]
\boldsymbol{\gamma}(z, +0) = \dfrac{1}{2\cos^2\theta}\begin{pmatrix} G - F\cos 2\theta & -2K\sin^2\theta \\ -2K\sin^2\theta & G\cos 2\theta - F \end{pmatrix}(z, +0) \\[4mm]
\boldsymbol{\delta}(z, +0) = \dfrac{1}{2\cos^2\theta}\begin{pmatrix} G + F & 2K \\ -2K & G + F \end{pmatrix}(z, +0)
\end{cases}
$$

The values $\mathbf{T}(z, +0)$ follows from (8.2) by integration along the z-axis. The result is, see also (B.5) in Appendix B

$$
v\mathbf{T}(z, +0) = \int_z^L \mathbf{Q}(z', z)\left\{\partial_s\boldsymbol{\alpha} - \boldsymbol{\beta}\boldsymbol{\gamma}/2\right\}(z', +0)\mathbf{Q}(z, z')\,dz'
$$

The finite jump discontinuity in $\mathbf{R}$ along the line $s = 2(L - z)/v$ is denoted by $[\mathbf{R}](z)$, i.e.,

$$
[\mathbf{R}](z) = \mathbf{R}(z, 2(L - z)/v + 0) - \mathbf{R}(z, 2(L - z)/v - 0)
$$

The discontinuity is found by standard propagation of singularity arguments, see [6], using (8.1). The result is, see also (B.6) in Appendix B

$$
\begin{aligned}
(z) = &\frac{1}{2}\exp\left\{\int_L^z \boldsymbol{\delta}(z', +0)\,\frac{dz'}{v}\right\}\boldsymbol{\gamma}(L, +0)\exp\left\{\int_z^L \boldsymbol{\alpha}(z', +0)\,\frac{dz'}{v}\right\} \\
= &\exp\left\{-\frac{1}{c\cos\theta}\int_z^L (G(z', +0) + F(z', +0))\,dz'\right\} \\
&\frac{1}{2}\begin{pmatrix} \cos\phi(z, L) & \sin\phi(z, L) \\ -\sin\phi(z, L) & \cos\phi(z, L) \end{pmatrix}\boldsymbol{\gamma}(L, +0)\begin{pmatrix} \cos\phi(z, L) & -\sin\phi(z, L) \\ \sin\phi(z, L) & \cos\phi(z, L) \end{pmatrix}
\end{aligned}
\tag{8.3}
$$

where $\phi(z, L)$ is given by (6.1).

The imbedding equations (8.1) and (8.2) both consist of a set of three and four coupled partial differential equations, respectively. The four entries in the matrix equation for the reflection imbedding equation are:

$$
\begin{cases}
v\partial_z R_{11} - 2\partial_s R_{11} = \partial_s \{ -\beta_{11} - 2\alpha_{11} * R_{11} + 2\alpha_{12} * R_{12} \\
\qquad - R_{11} * (\beta_{11} * R_{11} + \beta_{12} * R_{12}) - R_{12} * (\beta_{12} * R_{11} + \beta_{22} * R_{12}) \} \\
v\partial_z R_{12} - 2\partial_s R_{12} = \partial_s \{ \beta_{12} - (\alpha_{11} + \alpha_{22}) * R_{12} + \alpha_{12} * (R_{22} - R_{11}) \\
\qquad - R_{11} * (\beta_{11} * R_{12} + \beta_{12} * R_{22}) - R_{12} * (\beta_{12} * R_{12} + \beta_{22} * R_{22}) \} \\
v\partial_z R_{22} - 2\partial_s R_{22} = \partial_s \{ -\beta_{22} - 2\alpha_{22} * R_{22} - 2\alpha_{12} * R_{12} \\
\qquad - R_{12} * (\beta_{11} * R_{12} + \beta_{12} * R_{22}) - R_{22} * (\beta_{12} * R_{12} + \beta_{22} * R_{22}) \}
\end{cases}
$$

The corresponding entries in the matrix equation for the transmission imbedding equation are:

$$
\begin{cases}
v\partial_z T_{11} = \alpha_{11}(z, +0)T_{11} + \alpha_{12}(z, +0)T_{21} \\
\qquad - \partial_s \{ \alpha_{11} + \alpha_{11} * T_{11} - \alpha_{12} * T_{12} + \beta_{11} * R_{11} + \beta_{12} * R_{12} \\
\qquad + T_{11} * (\beta_{11} * R_{11} + \beta_{12} * R_{12}) + T_{12} * (\beta_{12} * R_{11} + \beta_{22} * R_{12}) \} \\
v\partial_z T_{12} = \alpha_{11}(z, +0)T_{12} + \alpha_{12}(z, +0)T_{22} \\
\qquad - \partial_s \{ \alpha_{12} + \alpha_{12} * T_{11} + \alpha_{22} * T_{12} + \beta_{11} * R_{12} + \beta_{12} * R_{22} \\
\qquad + T_{11} * (\beta_{11} * R_{12} + \beta_{12} * R_{22}) + T_{12} * (\beta_{12} * R_{12} + \beta_{22} * R_{22}) \} \\
v\partial_z T_{21} = -\alpha_{12}(z, +0)T_{11} + \alpha_{22}(z, +0)T_{21} \\
\qquad - \partial_s \{ -\alpha_{12} + \alpha_{11} * T_{21} - \alpha_{12} * T_{22} + \beta_{12} * R_{11} + \beta_{22} * R_{12} \\
\qquad + T_{21} * (\beta_{11} * R_{11} + \beta_{12} * R_{12}) + T_{22} * (\beta_{12} * R_{11} + \beta_{22} * R_{12}) \} \\
v\partial_z T_{22} = -\alpha_{12}(z, +0)T_{12} + \alpha_{22}(z, +0)T_{22} \\
\qquad - \partial_s \{ \alpha_{22} + \alpha_{12} * T_{21} + \alpha_{22} * T_{22} + \beta_{12} * R_{12} + \beta_{22} * R_{22} \\
\qquad + T_{21} * (\beta_{11} * R_{12} + \beta_{12} * R_{22}) + T_{22} * (\beta_{12} * R_{12} + \beta_{22} * R_{22}) \}
\end{cases}
$$

Note that to solve the transmission kernels T_{ij} the reflection kernels R_{ij} have to be known. Despite the complexity of these equations they are very well suited for numerical calculations. Numerical results are reported in a sequent paper.

9   The Imbedding equations at normal incidence

The imbedding equations in Section 8 give the equations for general oblique incidence. In general, the scattering problem is solved by a system of four coupled partial differential equations. In this section the simplifications that occur for normal incidence are explicitly pointed out.

At normal incidence, $\theta = 0$, equation (7.1) is simplified. Due to axial symmetry of the problem, the reflection and transmission kernels have only two independent entries and, furthermore, $\mathbf{S} = \mathbf{I}$ and $s = t$. The reflection and transmission kernels

for normal incidence are

$$\begin{cases} \boldsymbol{E}^-(z,t) = \left(\mathbf{R}(z,\cdot) * \boldsymbol{E}^+(z,\cdot)\right)(t) \\ \boldsymbol{E}^+(L, t + (L-z)/c) = \mathbf{Q}(z,L)\left\{\boldsymbol{E}^+(z,t) + \left(\mathbf{T}(z,\cdot) * \boldsymbol{E}^+(z,\cdot)\right)(t)\right\} \end{cases}$$

where

$$\mathbf{R}(z,t) = \begin{pmatrix} R_1(z,t) & -R_2(z,t) \\ R_2(z,t) & R_1(z,t) \end{pmatrix}$$

and

$$\mathbf{T}(z,t) = \begin{pmatrix} T_1(z,t) & -T_2(z,t) \\ T_2(z,t) & T_1(z,t) \end{pmatrix}$$

It is easy to see that all 2×2 matrices of this form commute.

The imbedding equations, (8.1) and (8.2), and the finite jump discontinuities simplify to

$$2c\partial_z\mathbf{R} - 4\partial_t\mathbf{R} = \partial_t\left\{\mathbf{G} - \mathbf{F} + 2(\mathbf{G}+\mathbf{F})*\mathbf{R} + (\mathbf{G}-\mathbf{F})*\mathbf{R}*\mathbf{R}\right\} \qquad (9.1)$$

$$\mathbf{R}(L,t) = \mathbf{0}$$

$$\mathbf{R}(z,+0) = -\frac{\mathbf{G}(z,+0) - \mathbf{F}(z,+0)}{4}$$

$$[\mathbf{R}](z) = \frac{\mathbf{G}(L,+0) - \mathbf{F}(L,+0)}{4}\exp\left\{-\int_z^L (G+F)(z',+0)\,\frac{dz'}{c}\right\}$$

for the reflection kernels, and for the transmission kernels the result is

$$\begin{aligned} 2c\partial_z\mathbf{T} &= \partial_t\left\{\mathbf{G}+\mathbf{F}+2\mathbf{K}\right\} + \partial_t\left\{\mathbf{G}+\mathbf{F}+2\mathbf{K}\right\}*\mathbf{T} \\ &\quad + \partial_t\left\{(\mathbf{G}-\mathbf{F})*(\mathbf{R}+\mathbf{R}*\mathbf{T})\right\} \end{aligned} \qquad (9.2)$$

$$\mathbf{T}(L,t) = \mathbf{0}$$

$$8c\mathbf{T}(z,+0) = \int_z^L \left\{(\mathbf{G}-\mathbf{F})^2 - 4\partial_t(\mathbf{G}+\mathbf{F}+2\mathbf{K})\right\}(z',+0)\,dz'$$

Notice that $\mathbf{G} = G\mathbf{I}$ and $\mathbf{F} = F\mathbf{I}$ for normal incidence. The domain of definition for these equations is $\{(z,t) : t > 0,\, 0 < z < L \text{ and } t \neq 2(L-z)/c\}$. Also note that $\mathbf{R} = \mathbf{0}$ if $\mathbf{G} = \mathbf{F}$.

Equation (9.1) shows that $R_2(z,t) = 0$, since the imbedding equation (9.1) has only diagonal entries and no off-diagonal terms (this assumes unique solubility of the equation). The reflection kernel then simplifies to $\mathbf{R}(z,t) = R_1(z,t)\mathbf{I} = R(z,t)\mathbf{I}$, where $\mathbf{I}$ is the 2×2 identity matrix. As a consequence of this, the cross-polarized part of the reflected electric field from the finite or semi-infinite (reciprocal) bi-isotropic slab will be zero even if the slab is inhomogeneous. This result holds for any susceptibility kernels G, F and K and is therefore a general result.

Finally, for completeness the explicit entries of the imbedding matrix equations (9.1) and (9.2) are given.

$$\begin{cases} 2c\partial_z R - 4\partial_t R = \partial_t\left\{G - F + 2(G+F)*R + (G-F)*R*R\right\} \\ 2c\partial_z T_1 = \partial_t\left\{G+F\right\}*T_1 - 2\partial_t\left\{K\right\}*T_2 + \partial_t\left\{G + F + (G-F)*(R+R*T_1)\right\} \\ 2c\partial_z T_2 = \partial_t\left\{G+F\right\}*T_2 + 2\partial_t\left\{K\right\}*T_1 + \partial_t\left\{2K + (G-F)*R*T_2\right\} \end{cases}$$

10   Homogeneous, semi-infinite slab

If the slab is homogeneous and semi-infinite, see Figure 4, $\mathbf{R}$ is independent of z so that equation (8.1) can be integrated (with respect to s). Hence, equation (8.1) simplifies to

$$2\mathbf{R} + \boldsymbol{\gamma} + \boldsymbol{\delta} * \mathbf{R} - \mathbf{R} * \boldsymbol{\alpha} - \mathbf{R} * \boldsymbol{\beta} * \mathbf{R} = \mathbf{0}, \quad s > 0 \tag{10.1}$$

or equivalently

$$\begin{cases} 2R_{11} - \beta_{11} - 2\alpha_{11} * R_{11} + 2\alpha_{12} * R_{12} \\ \quad - R_{11} * (\beta_{11} * R_{11} + \beta_{12} * R_{12}) - R_{12} * (\beta_{12} * R_{11} + \beta_{22} * R_{12}) = 0 \\ 2R_{12} + \beta_{12} - (\alpha_{11} + \alpha_{22}) * R_{12} + \alpha_{12} * (R_{22} - R_{11}) \\ \quad - R_{11} * (\beta_{11} * R_{12} + \beta_{12} * R_{22}) - R_{12} * (\beta_{12} * R_{12} + \beta_{22} * R_{22}) = 0 \\ 2R_{22} - \beta_{22} - 2\alpha_{22} * R_{22} - 2\alpha_{12} * R_{12} \\ \quad - R_{12} * (\beta_{11} * R_{12} + \beta_{12} * R_{22}) - R_{22} * (\beta_{12} * R_{12} + \beta_{22} * R_{22}) = 0 \end{cases}$$

These equations give the solution to scattering problem for a semi-infinite, homogeneous medium at oblique incidence. Notice that this is a system of non-linear Volterra equations of the second kind in $\mathbf{R}$. Equations of this kind are very stable and easy to solve numerically, see Ref. [20].

ϵ, μ ϵ, μ
$G(t) = 0$ $G(t) = 0$
$F(t) = 0$ $F(t) = 0$
$K(t) = 0$ $K(t) = 0$
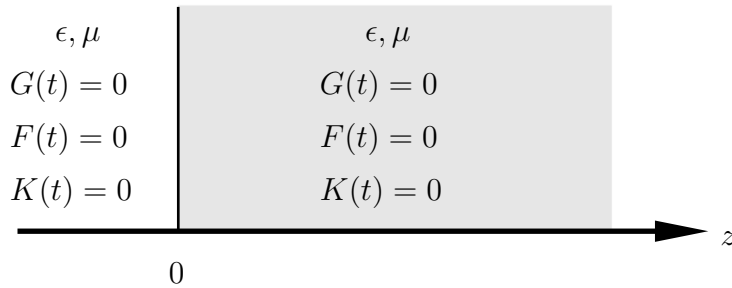
Figure 4:   Geometry of the semi-infinite slab problem.

Again, at normal incidence simplifications occur in (10.1). The reflection equation then reduces to

$$4R + G - F + 2(G + F) * R + (G - F) * R * R = 0, \quad t > 0$$

This result agrees with the result given in Ref. [20] for the case of $F(t) = 0$ (use the result of Appendix A).

The results in this section can also be used in the homogeneous but finite slab in the region $\{(z, s) : 0 < z < L \text{ and } 0 < s < 2(L - z)/v\}$. The effect of the back wall reflection is not effecting the reflection in the interval $0 < s < 2(L - z)/v$.

11 The Green Functions

In this section a different way of obtaining the scattering kernels is presented. The approach of Green functions was originally introduced by Krueger and Ochs [21] for the dispersionless case and by Kristensson [15] for the isotropic medium with dispersion. The method also gives the internal fields of the slab.

The Green functions $\mathbf{G}'^+(z,s)$ and $\mathbf{G}'^-(z,s)$ are defined for $(z,s) \in [0,L] \times (-\infty,\infty)$ through the relation between the fields $\boldsymbol{E}^+(z,s)$ and $\boldsymbol{E}^-(z,s)$ and the excitation $\boldsymbol{E}^+(0,s)$.

$$\begin{cases} \boldsymbol{E}^+(z,s+z/v) = \mathbf{Q}'(0,z)\boldsymbol{E}^+(0,s) + \left(\mathbf{G}'^+(z,\cdot) * \mathbf{Q}'(0,z)\boldsymbol{E}^+(0,\cdot)\right)(s) \\ \boldsymbol{E}^-(z,s+z/v) = \left(\mathbf{G}'^-(z,\cdot) * \mathbf{Q}'(0,z)\boldsymbol{E}^+(0,\cdot)\right)(s) \end{cases} \tag{11.1}$$

where

$$\left(\mathbf{G}'^\pm(z,\cdot) * \mathbf{Q}'(0,z)\boldsymbol{E}^+(0,\cdot)\right)(s) = \int_{-\infty}^s \mathbf{G}'^\pm(z,s-s') * \mathbf{Q}'(0,z)\boldsymbol{E}^+(0,s')\,ds'$$

and

$$\mathbf{G}'^\pm(z,s) = \begin{pmatrix} G_{11}^\pm(z,s) & G_{12}^\pm(z,s)/\cos\theta \\ G_{21}^\pm(z,s)\cos\theta & G_{22}^\pm(z,s) \end{pmatrix}$$

The Green functions are zero for $s < 0$ due to causality. The matrix $\mathbf{G}'^-$ has a finite jump discontinuity at $s = 2(L-z)/v$. The entries in the matrices $\mathbf{G}'^\pm$ are otherwise continuously differentiable functions for $s > 0$.

As in Section 8, it is convenient to introduce the following similarity transformation:

$$\mathbf{G}^\pm(z,s) = \mathbf{S}^{-1}\mathbf{G}'^\pm(z,s)\mathbf{S} = \begin{pmatrix} G_{11}^\pm(z,s) & G_{12}^\pm(z,s) \\ G_{21}^\pm(z,s) & G_{22}^\pm(z,s) \end{pmatrix}$$

It is easy to derive the following relationship between the imbedding and Green function formulations from their definitions, see (7.1) and (11.1):

$$\begin{cases} \mathbf{Q}(L,z)\mathbf{G}^+(L,s)\mathbf{Q}(z,L) = \mathbf{G}^+(z,s) + \mathbf{T}(z,s) + \left(\mathbf{T}(z,\cdot) * \mathbf{G}^+(z,\cdot)\right)(s) \\ \mathbf{G}^-(z,s) = \mathbf{R}(z,s) + \left(\mathbf{R}(z,\cdot) * \mathbf{G}^+(z,\cdot)\right)(s) \end{cases} \tag{11.2}$$

The boundary values are found analogously

$$\begin{cases} \mathbf{G}^+(0,s) = \mathbf{0} \\ \mathbf{G}^-(0,s) = \mathbf{R}(0,s) \\ \mathbf{G}^+(L,s) = \mathbf{Q}(0,L)\mathbf{T}(0,s)\mathbf{Q}(L,0) \\ \mathbf{G}^-(L,s) = \mathbf{0} \end{cases}$$

In the same way as the imbedding kernels, the Green functions $\mathbf{G}^\pm$ satisfy partial differential equations. Straightforward calculations give that, in the region $\{(z,s):$

$s > 0$, $0 < z < L$ and $s \neq 2(L-z)/v$}, the Green functions satisfy, see also (B.9) and (B.10) in Appendix B

$$v\partial_z \mathbf{G}^+ = -\mathbf{G}^+ \boldsymbol{\alpha}(z,+0) + \partial_s \left\{ \boldsymbol{\alpha} + \boldsymbol{\alpha} * \mathbf{G}^+ + \boldsymbol{\beta} * \mathbf{G}^- \right\} \tag{11.3}$$

$$v\partial_z \mathbf{G}^- - 2\partial_s \mathbf{G}^- = -\mathbf{G}^- \boldsymbol{\alpha}(z,+0) + \partial_s \left\{ \boldsymbol{\gamma} + \boldsymbol{\gamma} * \mathbf{G}^+ + \boldsymbol{\delta} * \mathbf{G}^- \right\} \tag{11.4}$$

$$\mathbf{G}^-(z,+0) = -\boldsymbol{\gamma}(z,+0)/2 = \mathbf{R}(z,+0)$$

where $\boldsymbol{\alpha}$, $\boldsymbol{\beta}$, $\boldsymbol{\gamma}$ and $\boldsymbol{\delta}$ are defined in (5.2), (5.3) and (5.4).

The value $\mathbf{G}^+(z,+0)$ can be obtained from (11.3) by integration. The result is

$$v\mathbf{G}^+(z,+0) = \int_0^z \mathbf{Q}(z',z) \left\{ \partial_s \boldsymbol{\alpha} - \boldsymbol{\beta}\boldsymbol{\gamma}/2 \right\} (z',+0) \mathbf{Q}(z,z') \, dz'$$

The finite jump discontinuity in $\mathbf{G}^-$ along the line $s = 2(L-z)/v$ is denoted $[\mathbf{G}^-](z)$, i.e.,

$$[\mathbf{G}^-](z) = \mathbf{G}^-(z, 2(L-z)/v + 0) - \mathbf{G}^-(z, 2(L-z)/v - 0)$$

The discontinuity is found from propagation of singularity arguments, or simpler from (11.2) and (8.3).

$$[\mathbf{G}^-](z) = \frac{1}{2} \exp \left\{ \int_L^z \boldsymbol{\delta}(z',+0) \, \frac{dz'}{v} \right\} \boldsymbol{\gamma}(L,+0) \exp \left\{ \int_z^L \boldsymbol{\alpha}(z',+0) \, \frac{dz'}{v} \right\} = [\mathbf{R}](z)$$

The Green function equations (11.3) and (11.4) are two coupled matrix equations. The entries of (11.3) are

$$\begin{cases}
v\partial_z G_{11}^+ = - \alpha_{11}(z,+0)G_{11}^+ + \alpha_{12}(z,+0)G_{12}^+ \\
\qquad + \partial_s \left\{ \alpha_{11} + \alpha_{11} * G_{11}^+ + \alpha_{12} * G_{21}^+ + \beta_{11} * G_{11}^- + \beta_{12} * G_{21}^- \right\} \\
v\partial_z G_{12}^+ = - \alpha_{22}(z,+0)G_{12}^+ - \alpha_{12}(z,+0)G_{11}^+ \\
\qquad + \partial_s \left\{ \alpha_{12} + \alpha_{11} * G_{12}^+ + \alpha_{12} * G_{22}^+ + \beta_{11} * G_{12}^- + \beta_{12} * G_{22}^- \right\} \\
v\partial_z G_{21}^+ = - \alpha_{11}(z,+0)G_{21}^+ + \alpha_{12}(z,+0)G_{22}^+ \\
\qquad + \partial_s \left\{ -\alpha_{12} + \alpha_{22} * G_{21}^+ - \alpha_{12} * G_{11}^+ + \beta_{22} * G_{21}^- + \beta_{12} * G_{11}^- \right\} \\
v\partial_z G_{22}^+ = - \alpha_{22}(z,+0)G_{22}^+ - \alpha_{12}(z,+0)G_{21}^+ \\
\qquad + \partial_s \left\{ \alpha_{22} + \alpha_{22} * G_{22}^+ - \alpha_{12} * G_{12}^+ + \beta_{22} * G_{22}^- + \beta_{12} * G_{12}^- \right\}
\end{cases}$$

and the corresponding entries of (11.4) are

$$\begin{cases}
v\partial_z G_{11}^- - 2\partial_s G_{11}^- = -\alpha_{11}(z,+0)G_{11}^- + \alpha_{12}(z,+0)G_{12}^- \\
\qquad + \partial_s \left\{ -\beta_{11} - \beta_{11} * G_{11}^+ + \beta_{12} * G_{21}^+ - \alpha_{11} * G_{11}^- + \alpha_{12} * G_{21}^- \right\} \\
v\partial_z G_{12}^- - 2\partial_s G_{12}^- = -\alpha_{22}(z,+0)G_{12}^- - \alpha_{12}(z,+0)G_{11}^- \\
\qquad + \partial_s \left\{ \beta_{12} - \beta_{11} * G_{12}^+ + \beta_{12} * G_{22}^+ - \alpha_{11} * G_{12}^- + \alpha_{12} * G_{22}^- \right\} \\
v\partial_z G_{21}^- - 2\partial_s G_{21}^- = -\alpha_{11}(z,+0)G_{21}^- + \alpha_{12}(z,+0)G_{22}^- \\
\qquad + \partial_s \left\{ \beta_{12} - \beta_{22} * G_{21}^+ + \beta_{12} * G_{11}^+ - \alpha_{22} * G_{21}^- - \alpha_{12} * G_{11}^- \right\} \\
v\partial_z G_{22}^- - 2\partial_s G_{22}^- = -\alpha_{22}(z,+0)G_{22}^- - \alpha_{12}(z,+0)G_{21}^- \\
\qquad + \partial_s \left\{ -\beta_{22} - \beta_{22} * G_{22}^+ + \beta_{12} * G_{12}^+ - \alpha_{22} * G_{22}^- - \alpha_{12} * G_{12}^- \right\}
\end{cases}$$

This system of equations is an alternative set of equations to solve the scattering problem. It is a system of eight coupled equations. However, the system is linear in contrast to the imbedding equations, which were non-linear, but only contained four coupled equations. Despite the complexity these equations are very well suited for numerical treatment, see also Ref. [20].

12   The Green Functions at normal incidence

Simplifications, similar to the ones found for the imbedding equations, occur at normal incidence. In this section these simplifications are explicitly pointed out.

At normal incidence equation (11.1) is transformed into ($\mathbf{S} = \mathbf{I}$ and $s = t$)

$$\begin{cases} \boldsymbol{E}^+(z, t + z/c) = \mathbf{Q}(0, z)\boldsymbol{E}^+(0, t) + \left(\mathbf{G}^+(z, \cdot) * \mathbf{Q}(0, z)\boldsymbol{E}^+(0, \cdot)\right)(t) \\ \boldsymbol{E}^-(z, t + z/c) = \left(\mathbf{G}^-(z, \cdot) * \mathbf{Q}(0, z)\boldsymbol{E}^+(0, \cdot)\right)(t) \end{cases}$$

where

$$\mathbf{G}^\pm(z, t) = \begin{pmatrix} G_1^\pm(z, t) & -G_2^\pm(z, t) \\ G_2^\pm(z, t) & G_1^\pm(z, t) \end{pmatrix}$$

due to axial symmetry. All 2×2 matrices of this form commute with each other.

The Green functions equations for normal incidence are

$$2c\partial_z \mathbf{G}^+ = (\mathbf{G}(z, +0) + \mathbf{F}(z, +0) + 2\mathbf{K}(z, +0))\mathbf{G}^+ \\ - \partial_t \left\{ \mathbf{G} + \mathbf{F} + 2\mathbf{K} + (\mathbf{G} + \mathbf{F} + 2\mathbf{K}) * \mathbf{G}^+ + (\mathbf{G} - \mathbf{F}) * \mathbf{G}^- \right\}$$

$$\mathbf{G}^+(0, t) = \mathbf{0}$$

$$8c\mathbf{G}^+(z, +0) = \int_0^z \left\{ (\mathbf{G} - \mathbf{F})^2 - 4\partial_t(\mathbf{G} + \mathbf{F} + 2\mathbf{K}) \right\}(z', +0) \, dz'$$

$\qquad\qquad\qquad\qquad\qquad\qquad\qquad\qquad\qquad\qquad$ (12.1)

for the matrix $\mathbf{G}^+$ and

$$2c\partial_z \mathbf{G}^- - 4\partial_t \mathbf{G}^- = (\mathbf{G}(z, +0) + \mathbf{F}(z, +0) + 2\mathbf{K}(z, +0))\mathbf{G}^- \\ + \partial_t \left\{ \mathbf{G} - \mathbf{F} + (\mathbf{G} - \mathbf{F}) * \mathbf{G}^+ + (\mathbf{G} + \mathbf{F} - 2\mathbf{K}) * \mathbf{G}^- \right\}$$

$$\mathbf{G}^-(L, t) = \mathbf{0}$$

$$\mathbf{G}^-(z, +0) = -\frac{1}{4}(\mathbf{G}(z, +0) - \mathbf{F}(z, +0))$$

$$[\mathbf{G}^-](z) = \frac{\mathbf{G}(L, +0) - \mathbf{F}(L, +0)}{4} \exp\left\{ -\int_z^L (G + F)(z', +0) \frac{dz'}{c} \right\}$$

$\qquad\qquad\qquad\qquad\qquad\qquad\qquad\qquad\qquad\qquad$ (12.2)

for the matrix $\mathbf{G}^-$. Notice that $\mathbf{G} = G\mathbf{I}$ and $\mathbf{F} = F\mathbf{I}$ for normal incidence. The region of definition in both these cases is $\{(z, t) : t > 0, 0 < z < L \text{ and } t \neq 2(L - z)/c\}$.

The explicit entries of the matrix equations (12.1) and (12.2) are

$$
\begin{cases}
2c\partial_z G_1^+ = \left\{ G(z,+0) + F(z,+0) \right\} G_1^+ - 2K(z,+0)G_2^+ \\
\qquad - \partial_t \left\{ G + F + (G+F) * G_1^+ - 2K * G_2^+ + (G-F) * G_1^- \right\} \\
2c\partial_z G_2^+ = \left\{ G(z,+0) + F(z,+0) \right\} G_2^+ + 2K(z,+0)G_1^+ \\
\qquad - \partial_t \left\{ 2K + (G+F) * G_2^+ + 2K * G_1^+ + (G-F) * G_2^- \right\} \\
2c\partial_z G_1^- - 4\partial_t G_1^- = \left\{ G(z,+0) + F(z,+0) \right\} G_1^- - 2K(z,+0)G_2^- \\
\qquad + \partial_t \left\{ G - F + (G-F) * G_1^+ + (G+F) * G_1^- + 2K * G_2^- \right\} \\
2c\partial_z G_2^- - 4\partial_t G_2^- = \left\{ G(z,+0) + F(z,+0) \right\} G_2^- + 2K(z,+0)G_1^- \\
\qquad + \partial_t \left\{ (G-F) * G_2^+ + (G+F) * G_2^- - 2K * G_1^- \right\}
\end{cases}
$$

The explicit relation between the imbedding kernels $\mathbf{R}$ and $\mathbf{T}$ and Green function formulations at normal incidence follows from equation (11.2).

$$
\begin{cases}
\mathbf{G}^+(L,t) = \mathbf{G}^+(z,t) + \mathbf{T}(z,t) + \left(\mathbf{T}(z,\cdot) * \mathbf{G}^+(z,\cdot) \right)(t) \\
\mathbf{G}^-(z,t) = R(z,t)\mathbf{I} + \left(R(z,\cdot) * \mathbf{G}^+(z,\cdot) \right)(t)
\end{cases}
$$

since all matrices commute. The kernels $\mathbf{T}(z,t)$ and $\mathbf{R}(z,t) = R(z,t)\mathbf{I}$ are the kernels introduced in Section 9.

Appendix A   Relation between constitutive relations

For the convenience of the reader an appendix with the transformation between the constitutive relation used in Ref. [20] and the present paper is given.

In Ref. [20] a slightly different set of constitutive relations was introduced.

$$
\begin{cases}
\boldsymbol{D}(\boldsymbol{r},t) = \epsilon_0\epsilon\left\{ \boldsymbol{E}(\boldsymbol{r},t) + (\mathcal{G} * \boldsymbol{E})(\boldsymbol{r},\sqcup) + \rfloor(\mathcal{K} * \boldsymbol{B})(\boldsymbol{r},\sqcup) \right\} \\
\boldsymbol{H}(\boldsymbol{r},t) = \epsilon_0\epsilon\left\{ c(\mathcal{K} * \boldsymbol{E})(\boldsymbol{r},\sqcup) + \rfloor^\in \left[\boldsymbol{B}(\boldsymbol{r},\sqcup) + (\mathcal{F} * \boldsymbol{B})(\boldsymbol{r},\sqcup) \right] \right\}
\end{cases}
$$

Specifically, in Ref. [20] these constitutive relations were introduced with $\mathcal{F} = 0$. The relation between this set of constitutive relations and the ones in (2.3) is given in terms of the resolvent of $\mathcal{F}(\boldsymbol{r},\sqcup)$.

$$
F + \mathcal{F} + \mathcal{F} * \mathcal{F} = \prime
$$

This is a Volterra equation of the second kind. The relation between the kernels $\mathcal{G}$, $\mathcal{F}$, $\mathcal{K}$ and G, F, K is easily found.

$$
\begin{cases}
G = \mathcal{G} - \mathcal{K} * \mathcal{K} = \mathcal{G} - \mathcal{K} * (\mathcal{K} + \mathcal{F} * \mathcal{K}) \\
K = \mathcal{K} + \mathcal{F} * \mathcal{K}
\end{cases}
$$

These equations can be used to transform the kernels $\mathcal{G}$, $\mathcal{F}$, $\mathcal{K}$ into the kernels G, F, K. Conversely, they can also be used to transform the kernels G, F, K into the kernels $\mathcal{G}$, $\mathcal{F}$, $\mathcal{K}$, by solving suitable Volterra equations of the second kind.

Appendix B   General equations

In this appendix the derivations of the imbedding equations and the Green function equations for a general 2×2 system are presented. The rotation and the attenuation of the wave front are also given.

The dynamics for a general 2×2 matrix system are assumed to be:

$$\frac{\partial}{\partial z} \begin{pmatrix} \boldsymbol{E}^+ \\ \boldsymbol{E}^- \end{pmatrix} = \frac{1}{c} \begin{pmatrix} -\mathbf{I} + \boldsymbol{\alpha}^+* & \boldsymbol{\beta}^-* \\ \boldsymbol{\beta}^+* & \mathbf{I} + \boldsymbol{\alpha}^-* \end{pmatrix} \frac{\partial}{\partial t} \begin{pmatrix} \boldsymbol{E}^+ \\ \boldsymbol{E}^- \end{pmatrix} \tag{B.1}$$

where the four 2×2 matrices $\boldsymbol{\alpha}^\pm$ and $\boldsymbol{\beta}^\pm$ are assumed to be continuous functions of space and time. The region of domain for this equation is $t \in (-\infty, \infty)$, $0 < z < L$ and the field $\boldsymbol{E}^-(L, t)$ is assumed to be zero. This last condition ensure that no sources are present on the right hand side of the slab.

Let $t^\pm \in (-\infty, \infty)$ and $0 < z^\pm < L$. Furthermore, assume there are finite jump discontinuities in the fields $\boldsymbol{E}^\pm$ along the lines $t = t^\pm \pm (z - z^\pm)/c$, respectively. The finite jump discontinuity in the field $\boldsymbol{E}^-$ is relevant if there is a phase velocity mismatch at the back wall of the slab. The finite jump discontinuity in $\boldsymbol{E}^\pm$ at (z, t) is denoted by square brackets $[\boldsymbol{E}^\pm(z, t)]$, i.e.,

$$[\boldsymbol{E}^\pm(z, t)] = \boldsymbol{E}^\pm(z, t + 0) - \boldsymbol{E}^\pm(z, t - 0)$$

Propagation of singularity arguments show that the finite jump discontinuities satisfy

$$\frac{d}{dz} \left[\boldsymbol{E}^\pm(z, t^\pm \pm (z - z^\pm)/c) \right] = \frac{1}{c} \boldsymbol{\alpha}^\pm(z, +0) \left[\boldsymbol{E}^\pm(z, t^\pm \pm (z - z^\pm)/c) \right]$$

The matrices $\boldsymbol{\beta}^\pm$ have no effect on the propagation of the discontinuities of the fields. Assume that the finite jump discontinuity in the slab is related to the jump at $z = z^\pm$ as

$$\left[\boldsymbol{E}^\pm(z, t^\pm \pm (z - z^\pm)/c) \right] = \mathbf{Q}^\pm(z^\pm, z) \left[\boldsymbol{E}^\pm(z^\pm, t^\pm) \right]$$

The matrix-valued functions $\mathbf{Q}^\pm(z^\pm, z)$ then satisfy

$$\begin{cases} \dfrac{d}{dz} \mathbf{Q}^\pm(z^\pm, z) = \dfrac{1}{c} \boldsymbol{\alpha}^\pm(z, +0) \mathbf{Q}^\pm(z^\pm, z) \\ \mathbf{Q}^\pm(z, z) = \mathbf{I} \\ \mathbf{Q}^\pm(z^\pm, z^\mp) = \mathbf{Q}^\pm(z, z^\mp) \mathbf{Q}^\pm(z^\pm, z) \end{cases}$$

The last equality implies that $\mathbf{Q}^\pm(z, z^\mp)$ as a function of its first argument satisfies

$$\frac{d}{dz} \mathbf{Q}^\pm(z, z^\mp) = -\frac{1}{c} \mathbf{Q}^\pm(z, z^\mp) \boldsymbol{\alpha}^\pm(z, +0)$$

Also note that

$$\mathbf{Q}^{\pm-1}(z^\mp, z) = \mathbf{Q}^\pm(z, z^\mp)$$

The imbedding kernels that relate the plus and the minus fields are defined by the following relations:

$$\begin{cases} \boldsymbol{E}^-(z,t) = \big(\mathbf{R}(z,\cdot) * \boldsymbol{E}^+(z,\cdot)\big)(t) \\ \boldsymbol{E}^+(L, t + (L-z)/c) = \mathbf{Q}^+(z,L)\big\{\boldsymbol{E}^+(z,t) + \big(\mathbf{T}(z,\cdot) * \boldsymbol{E}^+(z,\cdot)\big)(t)\big\} \end{cases} \tag{B.2}$$

In the region $\{(z,t) : t > 0,\, 0 < z < L \text{ and } t \neq 2(L-z)/c\}$ the imbedding kernels satisfy

$$\begin{cases} c\partial_z\mathbf{R} - 2\partial_t\mathbf{R} = \partial_t\big\{\boldsymbol{\beta}^+ + \boldsymbol{\alpha}^- * \mathbf{R} - \mathbf{R} * \boldsymbol{\alpha}^+ - \mathbf{R} * \boldsymbol{\beta}^- * \mathbf{R}\big\} \\ \mathbf{R}(L,t) = \mathbf{0} \\ \mathbf{R}(z,+0) = -\dfrac{1}{2}\boldsymbol{\beta}^+(z,+0) \end{cases} \tag{B.3}$$

and

$$\begin{cases} c\partial_z\mathbf{T} = \boldsymbol{\alpha}^+(z,+0)\mathbf{T} - \partial_t\big\{\boldsymbol{\alpha}^+ + \boldsymbol{\beta}^- * \mathbf{R} + \mathbf{T} * \boldsymbol{\alpha}^+ + \mathbf{T} * \boldsymbol{\beta}^- * \mathbf{R}\big\} \\ \mathbf{T}(L,t) = \mathbf{0} \end{cases} \tag{B.4}$$

These imbedding equations are found by differentiating (B.2) w.r.t. z and using the dynamics of the plus and minus fields in (B.1).

Evaluation of the imbedding equation for $\mathbf{T}$ at $t = 0$ and using the explicit value of the reflection kernel at $t = 0$ implies

$$c\partial_z\mathbf{T}(z,+0) = \boldsymbol{\alpha}^+(z,+0)\mathbf{T}(z,+0) - \mathbf{T}(z,+0)\boldsymbol{\alpha}^+(z,+0)$$
$$- \left\{\partial_t\boldsymbol{\alpha}^+(z,+0) - \frac{1}{2}\boldsymbol{\beta}^-(z,+0)\boldsymbol{\beta}^+(z,+0)\right\}$$

The reflection kernel has a finite jump discontinuity along the curve $t = 2(L-z)/c$. This discontinuity is denoted in square brackets, i.e.,

$$[\mathbf{R}](z) = \mathbf{R}(z, 2(L-z)/c + 0) - \mathbf{R}(z, 2(L-z)/c - 0)$$

The imbedding equation, (B.3), for the reflection kernel implies

$$c\frac{\mathrm{d}}{\mathrm{d}z}[\mathbf{R}](z) = \boldsymbol{\alpha}^-(z,+0)[\mathbf{R}](z) - [\mathbf{R}](z)\boldsymbol{\alpha}^+(z,+0)$$

From these equations it is easy to obtain

$$c\mathbf{T}(z,+0) = \int_z^L \mathbf{Q}^+(z',z)\left\{\partial_t\boldsymbol{\alpha}^+ - \frac{1}{2}\boldsymbol{\beta}^-\boldsymbol{\beta}^+\right\}(z',+0)\mathbf{Q}^+(z,z')\,dz' \tag{B.5}$$

and

$$[\mathbf{R}](z) = \mathbf{Q}^-(L,z))[\mathbf{R}](L)\mathbf{Q}^+(z,L) = \frac{1}{2}\mathbf{Q}^-(L,z)\boldsymbol{\beta}^+(L,+0)\mathbf{Q}^+(z,L) \tag{B.6}$$

respectively.

The imbedding kernels $\mathbf{R}$ and $\mathbf{T}$ relate the plus and minus fields at z (for transmission at $z = L$) to each other. The Green functions relate the plus and minus fields at z to the excitation at $z = 0$. The explicit definition of Green functions is

$$\begin{cases} \boldsymbol{E}^+(z, t + z/c) = \mathbf{Q}^+(0, z)\boldsymbol{E}^+(0, t) + \left(\mathbf{G}^+(z, \cdot) * \mathbf{Q}^+(0, z)\boldsymbol{E}^+(0, \cdot)\right)(t) \\ \boldsymbol{E}^-(z, t + z/c) = \left(\mathbf{G}^-(z, \cdot) * \mathbf{Q}^+(0, z)\boldsymbol{E}^+(0, \cdot)\right)(t) \end{cases} \quad \text{(B.7)}$$

The relation with the imbedding kernels and the Green functions is easily found by repeated use of (B.2) and (B.7).

$$\mathbf{Q}^+(L, z)\mathbf{G}^+(L, t)\mathbf{Q}^+(z, L) = \mathbf{G}^+(z, t) + \mathbf{T}(z, t) + \left(\mathbf{T}(z, \cdot) * \mathbf{G}^+(z, \cdot)\right)(t)$$
$$\mathbf{G}^-(z, t) = \mathbf{R}(z, t) + \left(\mathbf{R}(z, \cdot) * \mathbf{G}^+(z, \cdot)\right)(t) \quad \text{(B.8)}$$

The boundary values of the Green functions are also related to the scattering kernels of the problem.

$$\mathbf{G}^+(0, t) = \mathbf{0}$$
$$\mathbf{G}^-(0, t) = \mathbf{R}(0, t)$$
$$\mathbf{G}^+(L, t) = \mathbf{Q}^+(0, L)\mathbf{T}(0, t)\mathbf{Q}^+(L, 0)$$
$$\mathbf{G}^-(L, t) = \mathbf{0}$$

In the region $\{(z, t) : t > 0,\, 0 < z < L \text{ and } t \neq 2(L - z)/c\}$ the Green functions satisfy

$$c\partial_z \mathbf{G}^+ = -\mathbf{G}^+\boldsymbol{\alpha}^+(z, +0) + \partial_t \left\{\boldsymbol{\alpha}^+ + \boldsymbol{\alpha}^+ * \mathbf{G}^+ + \boldsymbol{\beta}^- * \mathbf{G}^-\right\} \quad \text{(B.9)}$$

and

$$\begin{cases} c\partial_z \mathbf{G}^- - 2\partial_t \mathbf{G}^- = -\mathbf{G}^-\boldsymbol{\alpha}^+(z, +0) + \partial_t \left\{\boldsymbol{\beta}^+ + \boldsymbol{\beta}^+ * \mathbf{G}^+ + \boldsymbol{\alpha}^- * \mathbf{G}^-\right\} \\ \mathbf{G}^-(z, +0) = -\dfrac{1}{2}\boldsymbol{\beta}^+(z, +0) = \mathbf{R}(z, +0) \end{cases} \quad \text{(B.10)}$$

These equations are found by differentiating (B.7) w.r.t. z and using the dynamics of the plus and minus fields in (B.1). Evaluation of (B.9) at $t = 0$ gives

$$c\partial_z \mathbf{G}^+(z, +0) = \boldsymbol{\alpha}^+(z, +0)\mathbf{G}^+(z, +0) - \mathbf{G}^+(z, +0)\boldsymbol{\alpha}^+(z, +0)$$
$$+ \left\{\partial_t \boldsymbol{\alpha}^+(z, +0) - \frac{1}{2}\boldsymbol{\beta}^-(z, +0)\boldsymbol{\beta}^+(z, +0)\right\}$$

It is then easy to obtain the value of $\mathbf{G}^+$ at $t = +0$.

$$c\mathbf{G}^+(z, +0) = \int_0^z \mathbf{Q}^+(z', z)\left\{\partial_t \boldsymbol{\alpha}^+ - \boldsymbol{\beta}^-\boldsymbol{\beta}^+/2\right\}(z', +0)\mathbf{Q}^+(z, z')\, dz'$$

The Green function $\mathbf{G}^-$ has a finite jump discontinuity along the line $t = 2(L - z)/c$. The discontinuity is denoted in square brackets.

$$[\mathbf{G}^-](z) = \mathbf{G}^-(z, 2(L - z)/c + 0) - \mathbf{G}^-(z, 2(L - z)/c - 0)$$

From (B.10) or (B.8), it follows that the explicit value of the discontinuity is

$$[\mathbf{G}^-](z) = \mathbf{Q}^-(L, z)[\mathbf{G}^-](L)\mathbf{Q}^+(z, L) = [\mathbf{R}](z) = \frac{1}{2}\mathbf{Q}^-(L, z)\boldsymbol{\beta}^+(L, +0)\mathbf{Q}^+(z, L)$$

Appendix Acknowledgment

References

[1] R.S. Beezley and R.J. Krueger. An electromagnetic inverse problem for dispersive media. *J. Math. Phys.*, **26**(2), 317–325, 1985.

[2] J.P. Corones, M.E. Davison, and R.J. Krueger. Direct and inverse scattering in the time domain via invariant imbedding equations. *J. Acoust. Soc. Am.*, **74**(5), 1535–1541, 1983.

[3] J.P. Corones, M.E. Davison, and R.J. Krueger. Wave splittings, invariant imbedding and inverse scattering. In A.J. Devaney, editor, *Inverse Optics*, pages 102–106, SPIE Bellingham, WA, 1983. Proc. SPIE 413.

[4] J.P. Corones and R.J. Krueger. Obtaining scattering kernels using invariant imbedding. *J. Math. Anal. Appl.*, **95**, 393–415, 1983.

[5] J.P. Corones, R.J. Krueger, and V.H. Weston. Some recent results in inverse scattering theory. In F. Santosa, Y. Pao, W. Symes, and C. Holland, editors, *Inverse Problems of Acoustic and Elastic Waves*, pages 65–81, SIAM Philadelphia, PA, 1985. Proc. SPIE 413.

[6] R. Courant and D. Hilbert. *Methods of Mathematical Physics*, volume 2. Interscience, New York, 1962.

[7] N. Engheta and D.L. Jaggard. Electromagnetic chirality and its applications. *IEEE Antennas and Propagation Society Newsletter*, pages 6–12, October 1988.

[8] S. He and A. Karlsson. Time domain Green functions technique for a point source over a dissipative stratified half-space. Technical Report TRITA-TET 91-1, Department of Electromagnetic Theory, S-100 44 Stockholm, Sweden, 1991.

[9] S. He and S. Ström. The electromagnetic scattering problem in the time domain for a dissipative slab and a point source using invariant imbedding: Reconstrucion of the permittivity and conductivity. Technical Report TRITA-TET 90-8, Department of Electromagnetic Theory, S-100 44 Stockholm, Sweden, 1990. *J. Comp. Appl. Math.* (in press).

[10] S. He and S. Ström. The electromagnetic scattering problem in the time domain for a dissipative slab and a point source using invariant imbedding. *J. Math. Phys.*, **32**(12), 3529–3539, 1991.

[11] A. Karlsson. Inverse scattering for viscoelastic media using transmission data. *Inverse Problems*, **3**, 691–709, 1987.

[12] A. Karlsson and G. Kristensson. Constitutive relations, dissipation and reciprocity for the Maxwell equations in the time domain. Technical Report LUTEDX/(TEAT-7005)/1–35/(1989), Lund Institute of Technology, Department of Electromagnetic Theory, P.O. Box 118, S-211 00 Lund, Sweden, 1989.

[13] A. Karlsson and G. Kristensson. Constitutive relations, dissipation and reciprocity for the Maxwell equations in the time domain. *J. Electro. Waves Applic.*, **6**(5/6), 537–551, 1992.

[14] K.L. Kreider. A wave splitting approach to time dependent inverse scattering for the stratified cylinder. *SIAM J. App. Math.*, **49**, 932–943, 1989.

[15] G. Kristensson. Direct and inverse scattering problems in dispersive media—Green's functions and invariant imbedding techniques. In Kleinman R., Kress R., and Martensen E., editors, *Direct and Inverse Boundary Value Problems*, Methoden und Verfahren der Mathematischen Physik, Band 37, pages 105–119, Mathematisches Forschungsinstitut Oberwolfach, FRG, 1991.

[16] G. Kristensson and R.J. Krueger. Direct and inverse scattering in the time domain for a dissipative wave equation. part 1: Scattering operators. *J. Math. Phys.*, **27**(6), 1667–1682, 1986.

[17] G. Kristensson and R.J. Krueger. Direct and inverse scattering in the time domain for a dissipative wave equation. part 2: Simultaneous reconstruction of dissipation and phase velocity profiles. *J. Math. Phys.*, **27**(6), 1683–1693, 1986.

[18] G. Kristensson and R.J. Krueger. Direct and inverse scattering in the time domain for a dissipative wave equation. part 3: Scattering operators in the presence of a phase velocity mismatch. *J. Math. Phys.*, **28**(2), 360–370, 1987.

[19] G. Kristensson and R.J. Krueger. Direct and inverse scattering in the time domain for a dissipative wave equation. part 4: Use of phase velocity mismatches to simplify inversions. *Inverse Problems*, **5**(3), 375–388, 1989.

[20] G. Kristensson and S. Rikte. Scattering of transient electromagnetic waves in reciprocal bi-isotropic media. *J. Electro. Waves Applic.*, **6**(11), 1517–1535, 1992.

[21] R.J. Krueger and R.L. Ochs, Jr. A Green's function approach to the determination of internal fields. *Wave Motion*, **11**, 525–543, 1989.

[22] A. Lakhtakia. Recent contributions to classical electromagnetic theory of chiral media: what next? *Speculations in Science and Technology*, **14**(1), 2–17, 1991.

[23] V.H. Weston. Invariant imbedding for the wave equation in three dimensions and the applications to the direct and inverse problems. *Inverse Problems*, **6**, 1075–1105, 1990.

[24] V.H. Weston. Time-domain wave-splitting of Maxwell's equations. Technical Report LUTEDX/(TEAT-7016)/1–25/(1991), Lund Institute of Technology, Department of Electromagnetic Theory, P.O. Box 118, S-211 00 Lund, Sweden, 1991.